Inorganic Chemistry

ARTICLE

pubs.acs.org/IC

Selective Anion Binding by a Cofacial Binuclear Zinc Complex of a Schiff-Base Pyrrole Macrocycle

Aline M. J. Devoille,[†] Patricia Richardson,[†] Nathan L. Bill,[‡] Jonathan L. Sessler,[‡,§] and Jason B. Love*[,†]

[†]EaStCHEM School of Chemistry, University of Edinburgh, The King's Buildings, West Mains Road, Edinburgh EH9 3JJ, U. K.

[‡]Department of Chemistry and Biochemistry, 1 University Station — A5300, The University of Texas Austin, Texas 78712-0165, United States

Supporting Information

ABSTRACT: The synthesis of the new cofacial binuclear zinc complex $[Zn_2(L)]$ of a Schiff-base pyrrole macrocycle is reported. It was discovered that the binuclear microenvironment between the two metals of $[Zn_2(L)]$ is suited for the encapsulation of anions, leading to the formation of $[K(THF)_6][Zn_2(\mu\text{-}Cl)(L)]\cdot 2THF$ and $[Bu^n{}_4N][Zn_2(\mu\text{-}OH)(L)]$ which were characterized by X-ray crystallography. Unusually obtuse Zn—X—Zn angles (X = Cl: 150.54(9)° and OH: 157.4(3)°) illustrate the weak character of these interactions and the importance of the cleft preorganization to stabilize the host. In the absence of added anion, aggregation of $[Zn_2(L)]$ was inferred and investigated by successive dilutions and by the addition of coordinating solvents to $[Zn_2(L)]$ solutions using NMR spectroscopy as well as isothermal microcalorimetry (ITC). On anion addition, evidence for deaggregation of $[Zn_2(L)]$, combined with the formation of the 1:1 host—guest complex, was observed by NMR spectroscopy and ITC titrations. Furthermore, $[Zn_2(L)]$ binds to Cl^- selectively in THF as deduced from the ITC analyses, while other halides induce only deaggregation. These conclusions were reinforced by density functional theory (DFT) calculations, which indicated that the binding energies of OH^- and Cl^- were significantly greater than for the other halides.

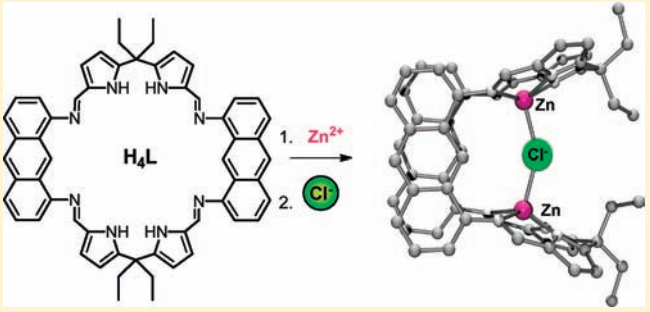

INTRODUCTION

The recognition and binding of anions such as halides, phosphates, and sulfate are key features of many biological processes, including those associated with information transmission, whereas a breakdown in the normal regulation of anion transport is implicated in several disease states, including cystic fibrosis.[1] A critical role for anion recognition is either recognized or proposed in a number of industrial processes, such as nuclear waste extraction and remediation,[2] as well as base and precious metal extraction.[3] Special attention has been given to metal-containing anion receptors as the metal center can play a crucial structural role in organizing anion-binding groups into a geometry appropriate for the recognition of a specific anion.[4−6] Furthermore, electrostatic interactions between the targeted anion and a Lewis acidic metal center can promote a binding event.[7,8] For example, in cascade complexes, first discovered by Lehn et al.,[9] a binucleating capsular ligand was used to accommodate two metallic centers within the cavity, typically in a *pseudo*-pyramidal geometry with a vacant site. These complexes, in which the two metallic centers are held at a well-defined distance from one another, can then recognize an anion of the appropriate size as the result of bridging coordination interactions involving the two metal centers. This principle has been further explored by several groups; in particular, Lu et al. found that dicobalt cryptates could be used to recognize selectively bromide and chloride over fluoride and iodide.[10] Separately, Fabrizzi et al. showed that halides, cyanides, azide, and hydroxide were encapsulated by a binuclear copper bis(tren) complex,[6] while McKee and Nelson discovered that azide and cyanide could be accommodated within a binuclear copper cryptate.[11] Other binuclear complexes in which the two metals adopt pyramidal geometries have been synthesized and have been shown to be capable of accommodating anions such as phosphates and their derivatives in bridging modes while in certain cases also acting as sensors.[8,12] While the detection of chloride using Lewis acidic late transition metal hosts remains relatively rare,[13] zinc porphyrins, species that are well-known to bind strong donor ligands,[14] have been shown to bind anions through electrostatic interactions.[5,15]

Cofacial or Pacman diporphyrins are a special class of porphyrins that combine the known coordinative properties of porphyrins with precise organization of the two metal binding sites through the use of a rigid, covalent link, so as to provide a binuclear microenvironment that is particularly well suited for small molecule redox chemistry.[16] The unique binuclear

Received: January 13, 2011
Published: March 10, 2011

Chart 1. Binuclear Pacman Complexes Derived from the Schiff-Base Pyrrole Macrocycle H_4L^o

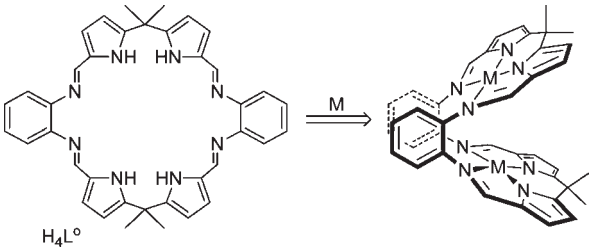

Scheme 1. Synthesis and Anion-Binding Reactions of the Binuclear Pacman Complex $[Zn_2(L)]$

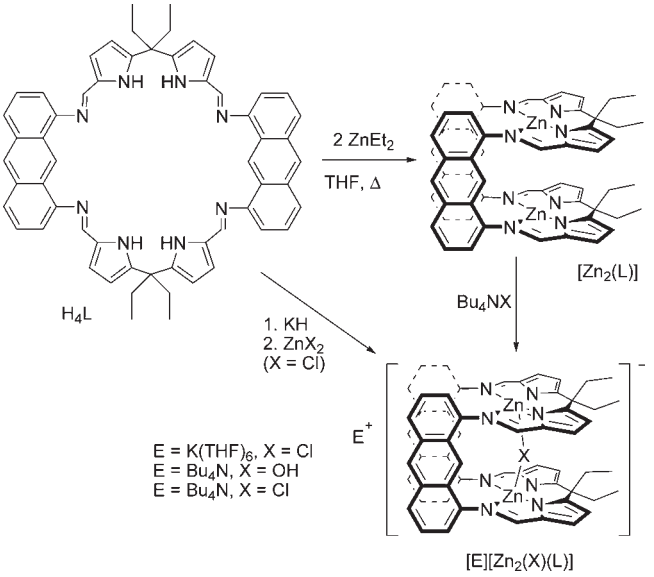

environment provided by these and other molecules created through the assembly of two metalloporphyrins, has been exploited in some aspects of host−guest chemistry. For example, using dimeric porphyrins, the recognition of molecules, such as DABCO,[17,18] and other bifunctional nitrogen donors, such as bipyridines, azides, anilines and diamines, has been successfully achieved.[18,19] Systems containing two zinc porphyrins have been designed to bind and signal the absolute configuration of diamines, aminoalcohols, and diols by exciton-coupled circular dichroism.[20] Also, increasing interest has been shown in the use of metallodiporphyrins to recognize larger molecules such as fullerenes.[21] Looking at the wide range of electron rich substrates that can be accommodated as guests, it is surprising that the anion-recognition ability of these systems remains largely unknown.

We developed recently a new approach to the formation of binuclear Pacman complexes that relies on the ability of the large, binucleating Schiff-base pyrrole macrocycles H_4L^o (Chart 1) to fold at aryl "hinges" upon metal coordination and so present a rigid binuclear microenvironment. These complexes were found to resemble structurally Pacman diporphyrins and to also carry out catalytic redox chemistry.[22] Furthermore, binuclear copper and cobalt complexes of L^o exhibited preferential in-cleft binding of a strong electron donor ligand such as pyridine, albeit with a distorted bonding mode because of the constrained space.[23] The modular nature and straightforward synthesis of H_4L^o allowed us to develop new macrocycles including H_4L (Scheme 1) in which the two MN_4 donor environments are separated by two anthracenyl hinges, a feature that allowed formation of the complex $[Pd_2(L)]$ in which the two metal compartments are cofacial with a Pd···Pd separation of 5.4 Å.[24] In this manuscript we report the synthesis and anion-binding properties of the new binuclear zinc complex $[Zn_2(L)]$ in which the zinc cations act both as structural agents to preorganize the ZnN_4 compartments into a cofacial binuclear microenvironment and as Lewis acids to accommodate an anion within the molecular cleft.

RESULTS AND DISCUSSION

Synthesis of $[Zn_2(L)]$. The reaction between H_4L and $ZnEt_2$ in hot tetrahydrofuran (THF) followed by the addition of diethyl ether affords the binuclear zinc complex $[Zn_2(L)]$ in good yield as an orange precipitate (Scheme 1). Even though the ^1H NMR spectrum of $[Zn_2(L)]$ is surprisingly complex and difficult to interpret, no obvious pyrrole NH resonances are seen, which is consistent with double-metalation of the macrocycle having occurred.

This conclusion is supported further by the IR spectrum, in which the N−H stretch is absent (normally observed at 3250 cm^{-1} in H_4L). In addition, a decrease in the C=N vibration from 1616 cm^{-1} (H_4L) to 1574 cm^{-1} upon metalation is seen. The nano-ESI mass spectrum in acetonitrile exhibits peaks with appropriate isotopic patterns, at m/z 1004 and 1068, corresponding to the water and bis-acetonitrile adducts $[Zn_2(L)]\cdot(H_2O)$ and $[Zn_2(L)]\cdot(CH_3CN)_2$, respectively; elemental analysis also supports the expected molecular composition. Unfortunately, and despite numerous attempts, crystals of $[Zn_2(L)]$ suitable for X-ray diffraction could not be grown, and so the solid state structure remains undetermined. However, the numerous resonances observed in the ^1H NMR spectrum of $[Zn_2(L)]$ combined with its poor solubility suggests that aggregation is occurring (see below).

Synthesis of the Binuclear Zinc Complex $[K(THF)_6][Zn_2(\mu\text{-}Cl)(L)]$. As an alternative synthetic route to $[Zn_2(L)]$, the reaction between K_4L and $ZnCl_2$ was carried out in THF and was found to generate the cofacial "ate" complex $[K][Zn_2(\mu\text{-}Cl)(L)]$. The ^1H NMR spectrum of $[K][Zn_2(\mu\text{-}Cl)(L)]$ displays the expected number of resonances, and the cofacial geometry of this complex was inferred from the nonequivalence of the endo- and exo-*meso*-ethyl substituents forming two overlapped quartets at 2.10 ppm and two triplets at 0.99 and 0.79 ppm; the nonequivalence of the ethyl groups was reinforced by appropriate resonances in the $^{13}C\{^1H\}$ NMR spectrum and assignments were confirmed by 2D NMR experiments. Unfortunately, bulk isolation of the product proved challenging because of the loss of THF solvent leading to apparent elimination of KCl. However, the slow evaporation of a THF solution of $[K][Zn_2(\mu\text{-}Cl)(L)]$ afforded a small quantity of crystals suitable for X-ray diffraction. The solid state structure of $[K(THF)_6][Zn_2(\mu\text{-}Cl)(L)]\cdot 2THF$ was determined and is shown in Figure 1, with crystal data and selected bond lengths and angles detailed in Supporting Information, Tables S1 and S2, respectively.

Consistent with what was inferred from an analysis of the solution NMR data, the complex adopts a double-pillared

dx.doi.org/10.1021/ic200082r |*Inorg. Chem.* 2011, 50, 3116–3126

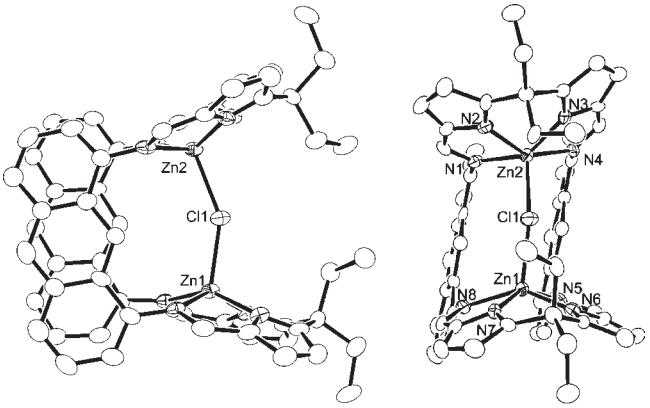

Figure 1. X-ray crystal structure of $[K(THF)_6][Zn(\mu\text{-}Cl)(L)]\cdot 2THF$ (displacement ellipsoids are drawn at 50% probability). For clarity, the $[K(THF)_6]^+$ cation, THF solvent of crystallization, and all hydrogen atoms are omitted.

cofacial structure in the solid state, with a zinc cation coordinated by each of the two N_4-donor pockets of the ligand. The accommodation of the chloride ion within the cleft forces the mouth to open resulting in the two N_4-donor planes deviating from coplanarity by 26.6°. In a similar manner to that observed in the solid state structure of the previously reported binuclear palladium complex $[Pd_2(L)]$,[24] the two anthracenyl backbones exist in a face-to-face arrangement with the π-surfaces stacked against one another. In this case, the shortest C-atom separation is 3.51(1) Å and the coplanarity of the aryl planes is high (3.0° deviation from the mean planes of the two anthracenes). The molecule is also C_2-twisted by an average of 13.8° between the N_4-donor plane and the anthracenyl backbone. The two zinc atoms, Zn1 and Zn2, are five coordinate and adopt pseudo-square pyramidal geometries with the Zn1 and Zn2 cations displaced into the cleft from the basal N_4-plane by 0.58 Å and 0.56 Å, respectively. This results in a Zn1···Zn2 separation of 4.532(1) Å, that is, about 0.9 Å shorter than in the $[Pd_2(L)]$ analogue. The chloride ion is symmetrically bridged between the two metal centers at distances of 2.340(2) Å and 2.346(2) Å from Zn1 and Zn2, respectively, and subtends a Zn1−Cl1−Zn2 angle of 150.54(9)°. The structure also includes an octahedral potassium cation coordinated by six molecules of THF.

The bimetallic complexes of H_4L can be considered as structural, and in some cases functional, double-pillared analogues of cofacial diporphyrins.[25] In this case, however, the structure of $[K(THF)_6][Zn_2(\mu\text{-}Cl)(L)]$ represents a unique example. Indeed, all known binuclear zinc diporphyrin complexes bind to the metals in a square planar geometry within the porphyrin plane and to the best of our knowledge, $[K(THF)_6][Zn_2(\mu\text{-}Cl)(L)]$ is the first X-ray solid state structure of a cofacial binuclear zinc complex with an anion bridging the two metals.[26] Furthermore, the presence of a bridging chloride anion is rare in polymetallic zinc chemistry, and the Zn1−Cl1−Zn2 angle of $[K(THF)_6][Zn_2(\mu\text{-}Cl)(L)]$ is unusually obtuse, being among the largest found in the Chemical Structural Database (mean 96.21°, range 71.53 to 179.97°, number of examples: 105).[27] This structural data leads us to suggest that the interaction between the Zn cations and the chloride anion is relatively weak and likely a direct consequence of the preorganization of the binuclear cleft, an inference that is fully consistent with the difficulties encountered in isolating this fragile compound.

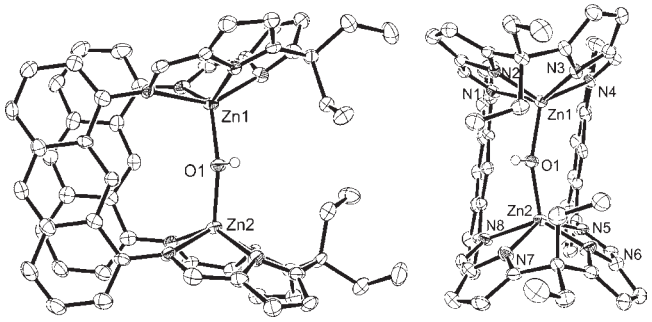

Figure 2. X-ray crystal structure of $[^nBu_4N][Zn_2(\mu\text{-}OH)(L)]$ (displacement ellipsoids are drawn at 50% probability). For clarity, the $^nBu_4N^+$ counterion and all hydrogen atoms except on the oxygen atom O1 are omitted.

Synthesis and Structure of $[^nBu_4N][Zn_2(\mu\text{-}OH)(L)]$. The reaction between $[Zn_2(L)]$ and 1 equiv of $^nBu_4NOH$ in THF generated the anion-bound complex $[^nBu_4N][Zn_2(\mu\text{-}OH)(L)]$. This complex that was characterized by ^1H NMR spectroscopy only and proved very difficult to isolate in a pure form. This outcome was ascribed to the hydrated and highly hygroscopic character of the hydroxide source which, according to the appearance of resonances for the unmetalated H_4L in the ^1H NMR spectrum, acts to decompose the $[Zn_2(L)]$ host. Nevertheless, in an attempt to synthesize $[^nBu_4N][Zn_2(\mu\text{-}F)(L)]$ from $[Zn_2(L)]$ and $^nBu_4NF$ in air, crystals of $[^nBu_4N][Zn_2(\mu\text{-}OH)(L)]$ were instead isolated. These proved suitable for X-ray diffraction analysis. The solid state structure was determined (Figure 2) and crystal data are detailed in Supporting Information, Table S1, with selected bond lengths and angles in Supporting Information, Table S2; refinement of the guest anion as fluoride led to a less satisfactory residual. Furthermore, the reaction between Li_4L and ZnI_2 did not generate the expected iodide-bridged complex $[Li][Zn_2(\mu\text{-}I)(L)]$ but instead crystals of $[Li(THF)_4][Zn_2(\mu\text{-}OH)(L)]\cdot 2THF$ were isolated from the reaction mixture. The X-ray crystal structure was determined and the zinc-ate core was found to be nearly identical to that of $[^nBu_4N][Zn_2(\mu\text{-}OH)(L)]$ so will not be discussed further (see Supporting Information, Figure S1). However, its elucidation provides support for the notion that the original complex, $[Zn_2(L)]$, binds hydroxide (presumably derived from a small quantity of water of crystallization) over fluoride.

The solid state structure of $[^nBu_4N][Zn_2(\mu\text{-}OH)(L)]$ reveals a hydroxyl group bridging the two zinc cations that adopt a geometrical arrangement similar to that seen in $[K(THF)_6]$-$[Zn_2(\mu\text{-}Cl)(L)]$. The two N_4-donor planes are found to deviate from coplanarity by 16.8°, and the π-stacking anthracenyl backbones exhibit a shortest C-atom separation of 3.322(8) Å with a displacement from coplanarity of 5.5°. The two zinc cations Zn1 and Zn2 are separated by 3.871(1) Å, that is, about 0.5 Å shorter than in the chloride-bridged analogue. The Zn-bridging hydroxide distances are 1.978(4) and 1.969(4) Å for Zn1−O1 and Zn2−O1, respectively. The bridge forms a Zn1−O1−Zn2 angle of 157.4(3)° which, as in the chloride analogue, is unusually obtuse, especially for a hydroxyl group bridged between two zinc cations and is the largest found in the literature (mean 111.13°, range 82.81 to 147.19°, number of examples: 137).[27] This feature again provides support for the inference that the cofacial structure is rigid and is unable to flex sufficiently to optimize the interaction between the zinc cations and the

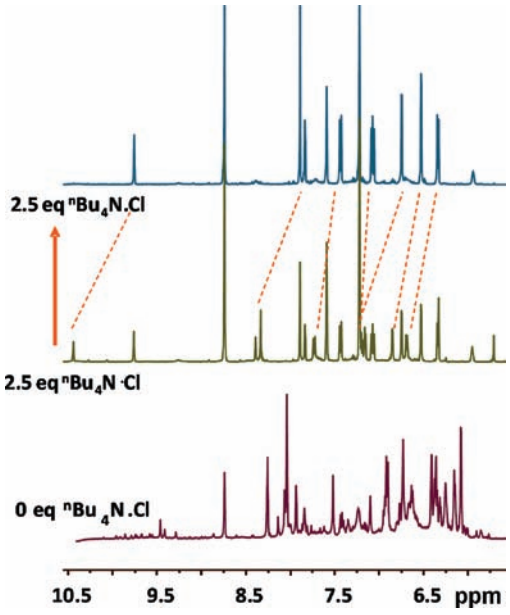

Figure 3. Reaction between $[Zn_2(L)]$ (16 mM) and $^nBu_4NCl$ in d_5-pyridine monitored over time by ^1H NMR spectroscopy (only the aromatic region shown).

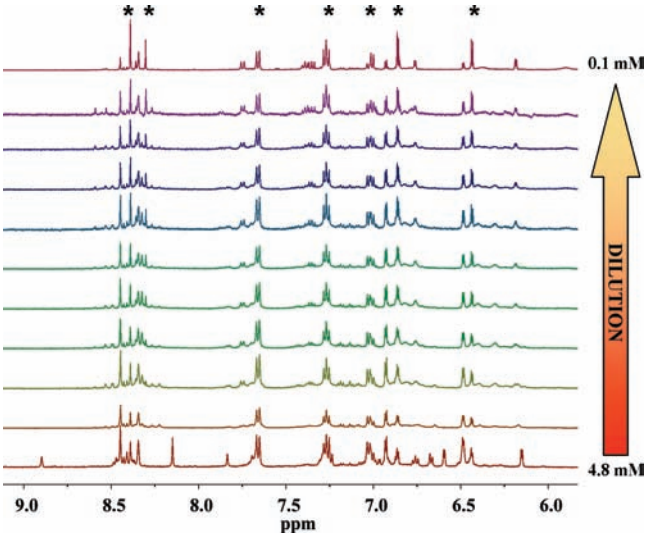

Figure 4. ^1H NMR spectra of $[Zn_2(L)]$ in THF recorded at concentrations ranging from 0.1 mM (top) to 4.8 mM (bottom). The stars indicate the position of the resonances of the monomeric species.

hydroxide anion. This conclusion is reinforced by the observation that, compared to $[K(THF)_6][Zn_2(\mu\text{-Cl})(L)]$, the two zinc cations are displaced even further into the cavity (N4 plane to Zn distance of 0.748 Å and 0.745 Å for Zn1 and Zn2, respectively) and the twist angle is smaller. These features may be a consequence of the steric clash between the *meso*-ethyl substituents and the fact that the two metals have to move within the cavity to obtain a small enough Zn···Zn separation to allow anion binding to occur. While all known binuclear zinc cofacial diporphyrins exhibit square planar geometries at the metal, the binuclear lutetium complex $[Lu_2(\mu\text{-OH})_2(DPA)]$ (where DPA is a single-anthracenyl-pillared diporphyrin) was shown by X-ray crystallography to have two hydroxyl anions bridging the two metals within the cavity in a manner similar to the "ate" complex $[Zn_2(\mu\text{-OH})(L)]^-$.[28] In the former Lu case, however, the increased size of Lu^{3+} (ionic radius 85 pm) compared to Zn^{2+} (74 pm), and the inability of the porphyrin to expand its N_4-donor cavity presumably leads to the observed out-of-plane binding of the Lu metal center and its corresponding propensity to stabilize bridging interactions with the cobound anions.

Solution Speciation and Anion Binding of $[Zn_2(L)]$. The isolation of zinc complexes of L that appear predisposed toward anion binding, coupled with the poor quality ^1H NMR data acquired for the parent binuclear zinc complex $[Zn_2(L)]$, encouraged us to evaluate possible aggregation and anion binding phenomena. With such a view in mind, the ability of $[Zn_2(L)]$ to bind chloride in solution was evaluated by ^1H NMR spectroscopy (Figure 3). The addition of an excess of $^nBu_4NCl$ to a solution of $[Zn_2(L)]$ caused the ^1H NMR spectrum to simplify considerably, leading immediately to signals that are ascribed to a mixture of two compounds. These signals resolve into a set of resonances consistent with the presence of only a single species over the course of 72 h. The presence of a double set of resonances at 2.91/2.45 and 1.41/1.12 ppm for the *meso*-ethyl substituents in the ^1H NMR spectrum recorded after 72 h is consistent with the formation of a complex of cofacial geometry, that is, the ultimate generation of $[^nBu_4N][Zn_2(\mu\text{-Cl})(L)]$. The second set of resonances seen in the ^1H NMR spectrum immediately on addition of Cl^- is consistent with a binuclear complex of cofacial structure and is likely due to the formation of monomeric $[Zn_2(L)]$, that is, the addition of Cl^- induces deaggregation.

Numerous examples of the self-assembly of zinc porphyrins have been reported that make use of the Lewis acidity of the zinc cation in these macrocyclic complexes, which is compensated by the addition of an extra ligand in the axial position.[14] Considering that the structural properties of cofacial Schiff-base pyrroles are similar to those of cofacial diporphyrins, the propensity of $[Zn_2(L)]$ to accept a strong donor ligand is likely and, in the absence of a suitable interaction, the underlying coordination deficiency that drives ligand association is compensated by aggregation. Although the interactions leading to the formation of aggregates and their speciation have not yet been determined, the consistent lack of resolution seen in the ^1H NMR spectra of $[Zn_2(L)]$ and the presence of some signals below 0 ppm are similar to those observed by Balaban and co-workers for the aggregation of zinc porphyrins.[29] To understand this aggregation process better, a sequential dilution study of $[Zn_2(L)]$ monitored by ^1H NMR spectroscopy was carried out in THF (Figure 4). On successive dilution from 4.8 to 0.1 mM gradual resolution toward a single set of signals is observed. These signals are identical to those seen above on addition of Cl^- and are consistent with the deaggregation to form monomeric $[Zn_2(L)]$ at lower concentrations. Better resolved signals are also seen in the ^1H NMR spectrum when the dilution experiment is carried out in a good donor solvent, such as pyridine. Such a finding is consistent with the intuitively reasonable expectation that the monomeric species is stabilized by the pyridine donor ligands.

Attempts to evaluate further the speciation of $[Zn_2(L)]$ in solution by UV−visible spectroscopy were hindered by its sensitivity toward protic impurities at the μM level and spectrophotometer saturation at mM concentrations. Furthermore, the addition of excess chloride to a THF solution of $[Zn_2(L)]$ made little change to the UV−visible spectrum, making it difficult to assign spectra to different species in solution (Supporting Information, Figure S3); as such, the solution speciation was

dx.doi.org/10.1021/ic200082r |*Inorg. Chem.* 2011, 50, 3116–3126

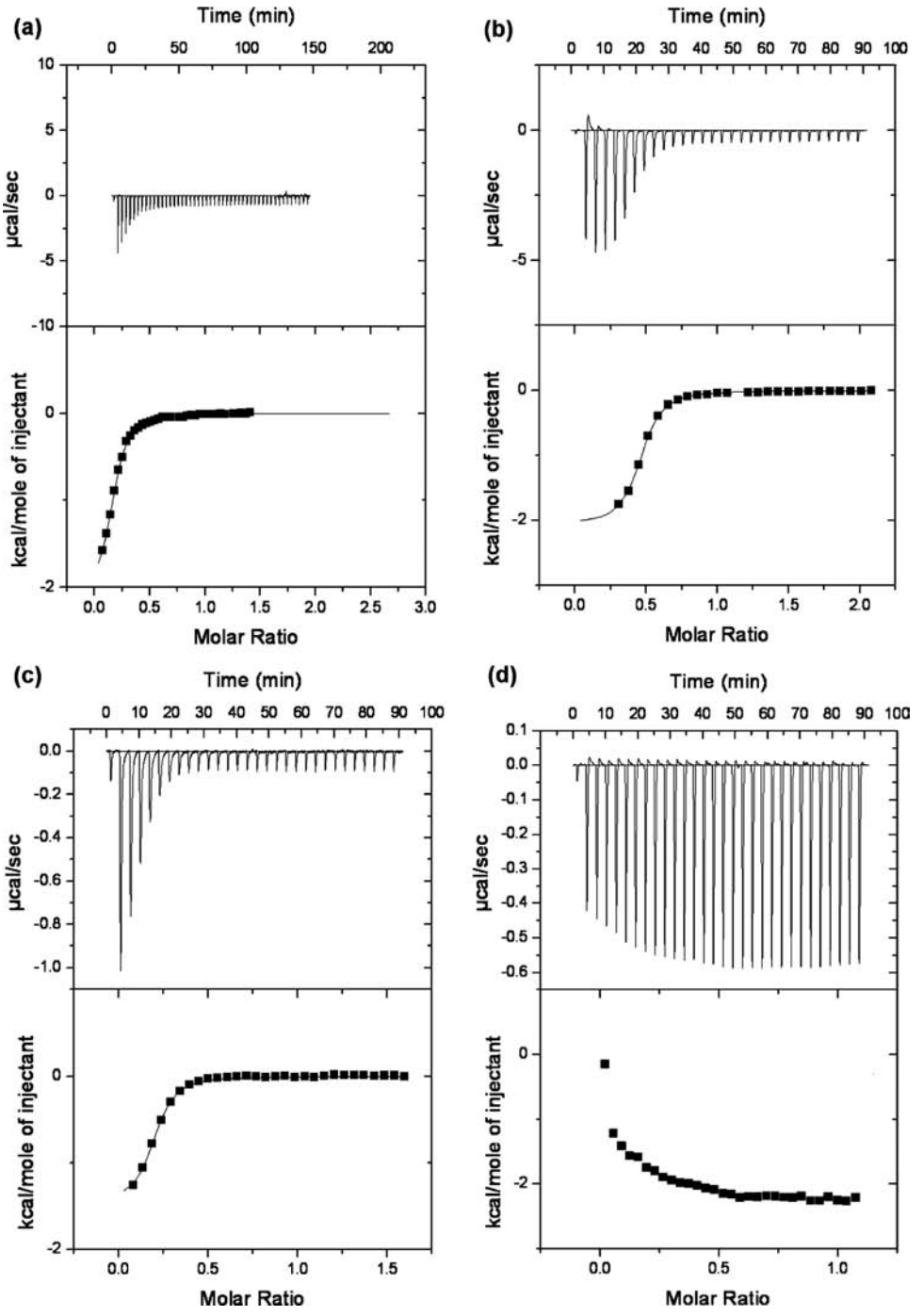

Figure 5. ITC traces corresponding to the titration of $[Zn_2(L)]$ with $^nBu_4NCl$ in DMF: (a) 50 °C, 1.12 mM, $n = 0.17$; (b) 25 °C, 0.67 mM, $n = 0.44$; (c) 25 °C, 0.34 mM, $n = 0.18$; (d) 25 °C, 0.13 mM, n = n/a.

studied by isothermal titration calorimetry (ITC) and NMR spectroscopy.

Each ITC experiment comprised the sequential addition of a solution of $[Zn_2(L)]$, which acts a host (Figure 5). The deaggregation phenomenon was studied using $^nBu_4NCl$ as an anion source and DMF the solvent. While $[Zn_2(L)]$ proved to be soluble enough to carry out ITC experiments in this solvent (DMF), no evidence of anion binding was observed. ITC experiments were also carried out at different temperatures and concentrations, and highlighted that more dilute and/or warmer samples required less anion to reach full dissociation, a finding that again supports the proposed aggregation/deaggregation of $[Zn_2(L)]$. Furthermore, at lower concentrations, that is, when full dissociation is achieved, a simple dilution pattern was observed.

Ideally, a solution of the fully deaggregated $[Zn_2(L)]$ would be required to carry out the anion binding studies. Unfortunately, a balance had to be found between the ability of a solvent to solvate $[Zn_2(L)]$ and its own binding ability, that is, a strong enough donor solvent is required to dissociate the aggregate but too good

dx.doi.org/10.1021/ic200082r |*Inorg. Chem.* 2011, 50, 3116–3126

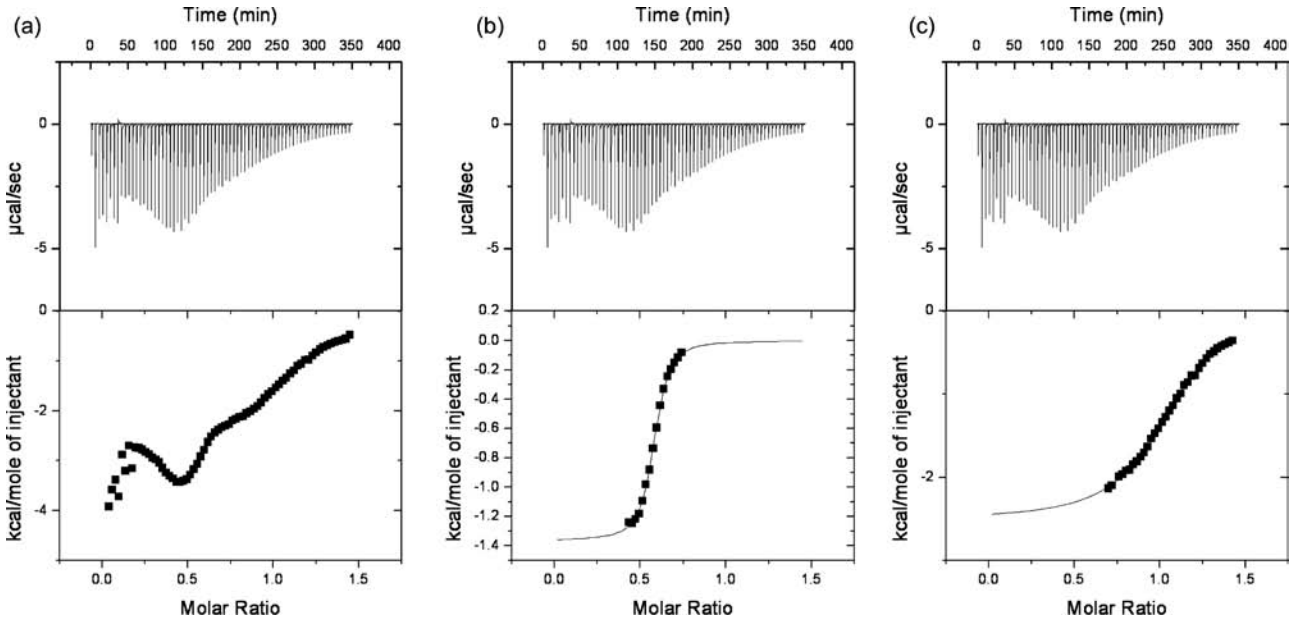

Figure 6. ITC traces of the titration of 1.11 mM $[Zn_2(L)]$ by 10.16 mM $^nBu_4NCl$ in THF: (a) full trace; (b) fitting profile for deaggregation phenomenon (n = 0.6); and (c) fitting profile for binding event (n = 1.1).

a donor binds strongly to the zinc centers of the metal complex, thereby competing with the anion binding event. Furthermore, the highly hygroscopic nature of the host complex required dry conditions to inhibit the formation of the hydroxyl-bridged species. Likewise, the presence of water could weaken significantly the strength of anion−metal cation interactions. Therefore, ^{1}H NMR anion binding experiments were carried out in THF or pyridine and care was taken to exclude moisture.

On sequential addition of $^nBu_4NCl$ the ^{1}H NMR spectrum of $[Zn_2(L)]$ in THF becomes more resolved and the signals for the chloride complex appear while the resonances for the free host vanish. This is just as is expected for a deaggregation event followed by anion binding (Supporting Information, Figure S2). Unfortunately, the aggregated nature of the host does not allow for accurate integration of the resonances. While this lack of precision precluded carrying out a Job plot analysis, a split of, for example, the signal for the 9*H*-anthracene proton from 9.65 ppm into 9.80 ppm and 9.16 ppm is seen to occur, as would be expected given this two step chemical transformation (i.e., deaggregation followed by anion−cation interaction). The same experiment carried out in pyridine-d_5 led to similar observations, in that two sets of well resolved signals were observed corresponding to the monomeric $[Zn_2(L)]$ from dilution and anion-bound $[Zn_2(\mu\text{-}Cl)(L)]^-$. As noted above, equilibration over 72 h afforded a single set of signals that are consistent with the formation of $[^nBu_4N][Zn(\mu\text{-}Cl)(L)]$ as the final, stable product. While such a conversion is consistent with all available data, the dynamic nature of the transformation renders quantitative measurements difficult using NMR spectroscopy. Therefore, we considered ITC to be a more useful method to investigate the proposed anion binding events.

ITC binding experiments were carried out in DMF and THF and focused on halides, which were studied in the form of their tetrabutylammonium salts (Figure 6). No reliable data were obtained for fluoride, possibly because of its hygroscopic nature and the potential for formation of a hydroxyl adduct. Therefore, fluoride ion was excluded from the study, and the investigations focused on chloride, bromide, and iodide. In DMF, the dissociation of the aggregate is observed on chloride addition but no evidence of binding was detected, leading us to suggest that DMF competes strongly with the anion at the binding site. The addition of bromide and iodide salts both lead to patterns typical of dilution only, which is consistent with their lower electronegativity and softer character compared to chloride. When a less coordinating solvent such as THF is used, changes consistent with deaggregation followed by anion binding of chloride are observed sequentially. Furthermore, the underlying data are consistent with a 1:1 binding event and are thus in full accord with the solid state data in which the anion is bound within the cavity of the Pacman-shaped molecule. The host complex $[Zn_2(L)]$ also exhibits selectivity for Cl^- over Br^- and I^- as only deaggregation phenomena are observed for the latter halides in THF solution. In all cases, it should be noted that only small quantities of heat were generated during deaggregation and anion-binding events and so reliable thermodynamic data were difficult to reproduce; typically, the deaggregation and binding events for Cl^- amount to 7.4 and 6.1 kcalmol^{-1}, respectively. Unfortunately, the poor solubility of $[Zn_2(L)]$ in THF limited the accessible concentration and therefore prevented the determination of more accurate values. The titrations were carried out at different host [H] and guest [G] concentration (at [H]/[G] of 1 mM/20 mM, 1 mM/10 mM and 0.5 mM/10 mM) and these variations did not affect the overall nature of the binding isotherms, thus providing important support for the proposed selective binding of chloride and with a 1:1 host:guest ratio (Table 1).

Calculations. DFT calculations were carried out to determine the structure of the binuclear zinc complex $[Zn_2(L)]$ and its propensity to act as a host for OH^-, Cl^-, Br^-, and I^- anions. The structure of the binuclear palladium complex $[Pd_2(L)]$ was used as a starting point for geometry optimization of $[Zn_2(L)]$ at the M05−2X/LANL2DZ level of theory. Bulk solvation effects were accounted for via the polarized continuum model (PCM), and the counterpoise method was use to correct for errors in the

dx.doi.org/10.1021/ic200082r |*Inorg. Chem.* 2011, 50, 3116–3126

Table 1. ITC Data in DMF and THF for the Titration of a 1.1 mM Solution of $[Zn_2(L)]$ by a 10 mM Solution of Anion

		deaggregation		binding	
anion	solvent	equivalence	K (M^{-1})	equivalence	K (M^{-1})
Cl^-	DMF	0.59	$111000 \pm 0.3 \times 10^4$	not observed	
Br^-	DMF	not observed		not observed	
I^-	DMF	not observed		not observed	
Cl^-	THF	0.58	$271000 \pm 1.5 \times 10^4$	1.07	$32200 \pm 1 \times 10^3$
Br^-	THF	0.73[a]	$41400 \pm 0.2 \times 10^4$	not observed	

[a] 20 mM guest solution.

Table 2. Comparison of Calculated and Experimental (Italicized) Structural Parameters and Counterpoise-Corrected, Solvated Anion Binding Energies for $[Zn_2(\mu\text{-}X)(L)]^-$ where X = OH, Cl, Br, I

	M···M (Å)	M−X−M (deg)	M o.o.p[a] (Å)	bite[b] (deg)	twist[c] (deg)	binding energy[d]/kcal mol^{-1}
$Zn_2(L)$	4.98	n/a	0.14	8.4	34.2	n/a
$Pd_2(L)$ exp[e]	*5.38*	*n/a*	*0.06*	*15.3*	*29.4*	*n/a*
$Zn_2(OH)(L)^-$	3.90	153.4	0.68	15.5	8.5	−49.3 (−31.8; −28.9)
$Zn_2(OH)(L)^-$ exp	*3.87*	*157.4*	*0.75*	*16.8*	*10.4*	*n/a*
$Zn_2(Cl)(L)^-$	4.68	150.5	0.54	28.9	11.2	−9.8 (+6.2; +5.9)
$Zn_2(Cl)(L)^-$ exp	*4.53*	*150.5*	*0.56*	*26.6*	*15.7*	*−6.1*[f]
$Zn_2(Br)(L)^-$	4.84	138.9	0.54	35.0	9.3	−4.0 (+11.0; +10.4)
$Zn_2(I)(L)^-$	5.03	130.1	0.53	40.7	8.8	+1.4 (+16.9; ----)

[a] o.o.p = distance of Zn out of N_4 donor plane into the cleft. [b] Dihedral angle subtended by the two N_4 donor planes. [c] Dihedral angle subtended by the N_4 donor plane and anthracenyl backbone. [d] M05−2X/LANL2DZ level of theory (B3LYP/LANL2DZ and B3LYP/6-31 g(d,p) successively in brackets), a negative value indicates anion-binding; [e] Ref 24. [f] Determined by ITC.

calculated binding energies of the anion-bound host−guest complexes $[Zn_2(X)(L)]^-$ arising from the incompleteness of the basis set. Absolute binding energies for the series of anions were determined and are detailed in Table 2 along with a comparison of geometrical data for experimental and calculated structures.

The substitution of Pd by Zn in the calculated structure of $[Zn_2(L)]$ causes significant changes to the gross molecular structure (Table 2). In particular, to incorporate the smaller cation the cofacial molecule adopts a significantly greater lateral twist (34.2° cf. 29.4° in $[Pd_2(L)]$) similar to that seen by us in the structural comparison of the *o*-phenylene-backbone-based complexes $[Pd_2(L^o)]$ and $[Ni_2(L^o)]$.[22] Furthermore, the $[Zn_2(L)]$ complex is more cofacial than its Pd counterpart (bite angles 8.4 vs 15.3° respectively), which results in a shortening of the Zn···Zn separation by 0.4 Å compared to the Pd analogue. Addition of the anion within the molecular cleft of $[Zn_2(L)]$ also causes significant structural changes; no exogenous binding of anion is seen. The calculated structure for $[Zn_2(OH)(L)]^-$ bears a close resemblance to the experimentally determined structure of $[Bu_4N][Zn_2(OH)(L)]$ with the Zn cations moving 0.68 Å into the cleft resulting in a Zn···Zn separation of 3.90 Å, an obtuse Zn−OH−Zn of 153.4° and a significantly reduced lateral twist angle of 8.5°. This latter angle is underestimated when compared to the experimental data which can be related to the essentially gas phase environment of the calculations compared to the condensed phase of the experimentally determined structure, which will be perturbed by crystal packing interactions. When the guest is chloride, the calculated structure is again similar to the experimental one, albeit with an underestimated lateral twist angle. The calculated structures for Br^- and I^- show that these anions are poorly accommodated by the macrocyclic complex. In particular, the bite angle is increased by 6° for Br^- and 12° for I^- which results in an increase in the Zn···Zn separation of 0.2 and 0.4 Å, respectively, and a concomitant decrease in the Zn−X−Zn angle by 10−20° as compared to the Cl^- and OH^- analogues. The lack of vertical expansion between the two ZnN_4 compartments contrasts to that seen in the porphyrinic analogues which are able to extend vertically from 3.5 to 7.8 Å. The difference is likely due to the presence of two anthracenyl pillars between the two compartments rather than the single pillar commonplace in Pacman diporphyrins. Comparison of the guest anion binding energies in the $[Zn_2(L)]$ host shows an important anion-dependency. In particular, the binding energy of OH^- is 5 times that of the most strongly interacting halide, Cl^-, and accounts for the experimentally observed propensity for the $[Zn_2(L)]$ host to scavenge hydroxyl from trace quantities of water present in the crystallization media. The calculated Cl^- binding energy at −9.8 kcalmol^{-1} is in reasonable agreement with that determined experimentally by ITC (−6.1 kcalmol^{-1}). The calculated binding energy of Br^-, at −4.0 kcal mol^{-1}, in light of the overestimation of the binding energy of Cl^- and coupled with the inherent error in the accuracy of the calculation method, is likely to correspond to a complex in which the anion is extremely weakly bound (>−1 kcalmol^{-1}), or is in fact unbound, as the I^- complex is predicted to be. Experimentally, this is supported by the ITC observation that Cl^- forms a 1:1 host:guest complex, while the addition of Br^- and I^- results only in dilution.

In the comparison of the three levels of theory, the calculated trends in the anion binding energies agree qualitatively with the trends observed experimentally (Table 2). Significantly stronger binding is observed for the hydroxide ion, than for the halides, which themselves show decreasing binding energies along the

dx.doi.org/10.1021/ic200082r |*Inorg. Chem.* 2011, 50, 3116–3126

series $Cl^- > Br^- > I^-$. Interestingly B3LYP, irrespective of the basis set used, predicts each of the halide-ligand complexes to be unbound, disagreeing with that seen experimentally. It is likely that the underestimation of the binding energies calculated with B3LYP is a direct result of its improper description of dispersive interactions. In contrast, the binding energies calculated with M05−2X/LANL2DZ are in much better agreement with the available experimental measurements.

CONCLUSIONS

The anthracenyl-hinged Schiff-base pyrrole macrocycle H_4L proved to be suitable for the complexation of two zinc cations, and the resulting complex $[Zn_2(L)]$ was characterized together with two of its "ate" compounds in which a chloride or hydroxide anion bridges the two metals within the binuclear cofacial molecular cleft. The anion-free complex $[Zn_2(L)]$ was found to be an aggregate in solution, and its dissociation was observed as a result of dilution, heating, or upon addition of certain anions. Significantly, in an appropriate solvent, $[Zn_2(L)]$ was found to accommodate selectively a chloride anion over the other halides as inferred from ITC experiments, while evidence of favored hydroxyl binding was also obtained. These host−guest interactions were found to be weak, a result that was corroborated by DFT calculations. These latter data revealed a distinct preference for hydroxide over chloride in the case of complex $[Zn_2(L)]$, and confirmed the experimentally observed finding that bromide and iodide give rise to much less thermodynamically stable host−guest interactions. The binding energy for $[Zn_2(\mu\text{-}Cl)(L)]^-$ calculated at the M05−2X/LANL2DZ level of theory was in good agreement with the experimental binding energy determined using ITC. Comparison with calculations at different levels of theory highlighted the importance of selecting a functional that includes a realistic description of midrange correlation when investigating the binding in neutral-anionic noncovalent complexes. It is clear from this work that the preformed, cofacial arrangement of Lewis acidic zinc cations facilitates the weak binding of small anions such as hydroxide and chloride within the molecular cleft; as such, wider investigations are planned to evaluate the effect of this binding event on the spectroscopic properties of these materials. In fact, preliminary results have been obtained that show that $[Zn_2(L)]$ also acts as a receptor for tetrahedral ions such as phosphate and thus may have a broader role to play as an anion recognition and sensing system. The flexible nature of the complex and the ability to respond to various stimuli in different chemical terms, that is, deaggregation vs anion binding lead us to suggest that the complex $[Zn_2(L)]$ and its analogues could be employed as a chemically controlled switching element.

EXPERIMENTAL SECTION

General Procedures. The synthesis of H_4L was carried out as described in the literature,[24] while all other chemicals were used as purchased. With the exception of $[Bu_4N][Zn_2(\mu\text{-}OH)(L)]$, all the zinc complexes were synthesized under nitrogen using Schlenk and glovebox techniques. Dry solvents (THF, DMF, toluene, and diethylether) were purified by passage through Vacuum Atmospheres solvent drying towers, pyridine was distilled from potassium and stored over molecular sieves, pyridine-d_5 and benzene-d_6 were dried over potassium, trap-to-trap vacuum distilled, and freeze−pump−thaw degassed three times. ^{1}H NMR spectra were recorded at 298 K on a Bruker ARX250, DPX360, DMX500, or AVA600 spectrometer operating at 250.13, 360.13, 500.13, and 599.81 MHz respectively; ^{13}C NMR spectra were recorded at 298 K on a Bruker ARX250, DPX360 or DMX500 spectrometer operating at 62.90, 90.55, and 125.77 respectively. Dilution experiments and titrations were recorded on a Bruker DMX500 spectrometer. All NMR spectra were referenced to residual protio-solvent resonances. When the solvent is THF, the ^{1}H NMR experiment was recorded with double-presaturation of THF with a small quantity of benzene-d_6 added as a deuterium lock. IR spectra were recorded on a JASCO FT/IR 460 Plus spectrometer in the range 4000−400 cm^{-1}. The UV−vis spectrum of $[Zn_2(L)]$ in THF was recorded on a PerkinElmer Lambda 9 UV/vis/NIR Spectrophotometer. The mass spectrum of $[Zn_2(L)]$ was recorded on a Q-Tof 2 (Micromass Waters Corporation, Manchester, U.K.) mass spectrometer using a nanoelectrospray ionization source, and its elemental analysis was carried out by Mr. Stephen Boyer at the London Metropolitan University. Microcalorimetric titrations were carried out using a MicroCal VP-ITC instrument and were processed with the Origin software provided.

Synthesis of $[Zn_2(L)]$. A solution of 1.1 M diethyl zinc in toluene (3.5 mL, 3.85 mmol) was added dropwise to a solution of H_4L (1 g, 1.16 mmol) in THF (10 mL) at −78 °C, allowed to reach room temperature and heated to reflux for 16 h. The orange suspension was treated with diethyl ether (20 mL) and the supernatant decanted by cannula transfer. The resulting orange solid was washed with diethyl ether (20 mL) and dried under vacuum (0.584 g, 51%).

^{1}H NMR (pyridine-d_5, 500.13 MHz): Broad overlapping resonances in the range 10−0.5 ppm.

IR (nujol): ν 1610 (w), 1574 (*C*═*N*), 1546 (*C*═*C*) cm^{-1}.

UV−vis (THF, 12 μM): λ_{max} 238 nm (ln ε = 10.59), 266 (10.85), 359 (10.52), 434(10.48).

Nano-ESI-MS: 1068 ($[M + 82]^+$, <1%, bis-MeCN adduct), 1004 ($[M+18]^+$, 2.5%, H_2O adduct), 861 ($[M - 2\ Zn + 1]^+$, 15%, ligand), 803 ($[M- 2\ Zn - 58]^+$, 74%, double Et loss on ligand), 429 ($[(M - 2Zn)]^{2+}/2$, 33%, ligand), 413 ($[(M - 2Zn) - 34]^{2+}/2$, 33%, double Me loss on ligand, doubly charged species)

Analysis. Found: C, 70.41; H, 4.84; N, 11.23. $C_{58}H_{48}N_8Zn_2$ requires: C,70.52; H, 4.90; N, 11.34%

Synthesis of $[K][Zn_2(\mu\text{-}Cl)(L)]$. THF (10 mL) was added to a stirred mixture of H_4L (0.200 g, 0.23 mmol) and KH (0.044 g, 1.15 mmol, 5 equiv) at −78 °C and allowed to reach room temperature. After 4 h, the resulting solution was added dropwise to a solution of $ZnCl_2$ (0.063 g, 0.46 mmol) in THF (1 mL) at room temperature. The red solution turned yellow almost instantly, and a solid appeared. The resulting mixture was stirred for 16 h after which the reaction mixture consisted of a thick suspension. Complete filtration was prevented by the very fine solid, and NMR data were recorded directly from the liquors.

^{1}H NMR (THF/benzene-d_6, 500.13 MHz): δ_H 8.91 (s, 2H, Ar*H*), 7.67 (br, 4H, imino), 7.64 (br, 2H, Ar*H*), 7.20 (d, 4H, *J* = 8.4 Hz, Ar*H*), 6.84 (t, 4H, *J* = 8.4 Hz, Ar*H*), 6.44 (d, 4H, *J* = 3.3 Hz, pyrrole C*H*), 6.33 (d, 4H, *J* = 6.8 Hz, Ar*H*), 6.08 (d, 4H, *J* = 3.3 Hz, pyrrole C*H*), 2.10 (two superimposed q, 8H, *J* = 7.1 Hz, CH_2), 0.99 (t, 6H, *J* = 7.2 Hz, CH_3), 0.79 (t, 6H, *J* = 7.3 Hz, CH_3).

^{13}C{^{1}H} NMR (THF/benzene-d_6 125.77 MHz): δ_C 157.2 (s, imino), 156.0 (s, quaternary), 151.2 (s, quaternary), 134.9 (s, quaternary), 132.0 (s, quaternary), 127.1 (s, quaternary), 126.4 (s, *C*H), 125.1 (s, *C*H), 125.0 (s, *C*H), 120.3 (s, *C*H), 117.3 (s, *C*H), 116.7 (s, *C*H), 111.4 (s, *C*H), 47.3 (s, CH_2), 39.2 (s, CH_2), 10.7 (s, CH_3) 9.90 (s, CH_3). Note: resonance due to *meso*-quaternary carbon is obscured by resonances due to THF.

Synthesis of $[^nBu_4N][Zn_2(\mu\text{-}Cl)(L)]$. N-tetrabutylammonium chloride (28 mg, 0.1 mmol) was added to a suspension of $[Zn_2(L)]$ (10 mg, 0.01 mmol) in pyridine-d_5, and the system was allowed to equilibrate for 64 h during which full dissolution of the sample occurred.

^{1}H NMR (pyridine-d_5, 500.13 MHz): δ_H 9.79 (s, 2H, Ar*H*), 7.89 (s, 4H, imino), 7.83 (s, 2H, Ar*H*), 7.43 (d, 4H, *J* = 8.5 Hz, Ar*H*), 7.07 (dd,

dx.doi.org/10.1021/ic200082r |*Inorg. Chem.* 2011, 50, 3116–3126

4H, J = 7.0 and 8.0 Hz, ArH), 6.75 (d, 4H, J = 3.3 Hz, pyrrole CH), 6.53 (d, 4H, J = 3.3 Hz, pyrrole CH), 6.34 (d, 4H, J = 6.8 Hz, ArH), 3.67 (m, free ^{n}Bu$_4$NCl), 2.91 (m, 4H, CH_2), 2.45 (m, 4H, CH_2), 1.88 (m, free ^{n}Bu$_4$NCl), 1.41 (t, 6H, J = 7.22 Hz, CH_3), 1.34 (m, free ^{n}Bu$_4$NCl), 1.12 (t, 6H, J = 7.53 Hz, CH_3), 0.88 (t, J = 7.3 Hz, free ^{n}Bu$_4$NCl). Resonances of the $[^n$Bu$_4$N$]^+$ countercation of $[$Zn$_2(\mu$-Cl)L$]^-$ overlap with the resonances for free ^{n}Bu$_4$NCl.

UV−vis (THF, 12 μM): λ_{max} 257 (ln ε = 10.54), 351 (9.79), 367 (9.78), 435 (9.70).

Synthesis of [^{n}Bu$_4$N][Zn$_2(\mu$-OH)(L)]. Solid ^{n}Bu$_4$NOH·30H$_2$O (74 mg, 0.09 mmol) was added to a suspension of [Zn$_2$(L)] (50 mg, 0.05 mmol) in THF (5 mL) at room temperature, and the mixture stirred for 48 h during which time full dissolution of the solids occurred. The solvent volume was reduced to 0.5 mL under reduced pressure, Et$_2$O (20 mL) was added, and the orange precipitate that formed was isolated, washed with Et$_2$O (5 mL), and dried under vacuum to yield [^{n}Bu$_4$N][Zn$_2(\mu$-OH)(L)] as an orange solid (37 mg, 57%).

^{1}H NMR (600 MHz, THF/benzene-d_6): δ_H 9.28 (s, 2H, ArH), 7.70 (s, 4H, imino), 7.60 (s, 2H, ArH), 7.21 (d, J = 8.4 Hz, 4H, ArH), 6.91 (m, 4H, ArH), 6.40 (d, J = 3.3 Hz, 4H, pyrrolic ArH), 6.32 (d, J = 6.7 Hz, 4H, ArH), 6.14 (d, J = 3.3 Hz, 4H, pyrrolic ArH), 2.81 (br, 15H, ^{n}Bu$_4$N), 2.49 (m, 4H, CH$_2$), 2.25 (m, 4H, CH$_2$), 1.26 (t, J = 7.2 Hz, 6H, CH$_3$), 1.09 (br.m, 40H, ^{n}Bu$_4$N), 0.89 (t, J = 7.3 Hz, 6H, CH$_3$), 0.676 (br.m, 52H, ^{n}Bu$_4$N). No resonances were observed for the hydroxyl proton, which may be obscured by the THF-suppression.

Over time, [^{n}Bu$_4$N][Zn$_2(\mu$-OH)(L)] reacts with water (solvent of crystallization from ^{n}Bu$_4$NOH·30H$_2$O or from the atmosphere) and demetalation of the complex occurs. This prevented the isolation of a high purity sample of [^{n}Bu$_4$N][Zn$_2(\mu$-OH)(L)], and repeated attempts at obtaining satisfactory elemental analytical data proved unsuccessful.

Crystallographic Details. X-ray diffraction data on single crystals of [K][Zn$_2(\mu$-Cl)(L)] and [^{n}Bu$_4$N][Zn$_2(\mu$-OH)(L)] were collected at 150 K on a Bruker SMART 1000 diffractometer equipped with a CCD area detector using graphite monochromated using Mo Kα radiation (λ= 0.71073 Å). Details of each data collection and refinement are given in Supporting Information, Table S1. The structures were solved by direct methods and refined by full-matrix least-squares refinement on $|F|^2$ using SHELXTL-97. All non-hydrogen atoms were refined with anisotropic displacement parameters while hydrogen atoms were placed at calculated positions and included as part of the riding model. The bridging hydroxyl hydrogen atom H001 was located using a 2-site free-variable refinement procedure and refined with fixed thermal parameters. The data for both [K][Zn$_2(\mu$-Cl)(L)] and [^{n}Bu$_4$N][Zn$_2(\mu$-OH)(L)] were weak, presumably because of facile desolvation of the crystal, and so have resulted in relatively high residuals. For [K][Zn$_2(\mu$-Cl)(L)], θ_{max} was lowered to prevent noise collection and some atoms in disordered molecules of THF could not be modeled satisfactorily. For [^{n}Bu$_4$N][Zn$_2(\mu$-OH)(L)], the relatively high residual electron density was located close to the Zn1 (0.9 Å) and is not at a sensible position for a hydrogen atom on the bridging hydroxide. Other high residual electron density was located close to Zn2.

^{1}H NMR Spectroscopic Dilution Experiments and Titrations. The dilution experiment was carried out using a 5 mM sample of [Zn$_2$(L)] in dry THF-d_8 with successive dilutions down to 0.1 mM. To ensure a suitable signal-to-noise in the ^{1}H NMR spectra, the number of scans was increased accordingly. NMR titrations were carried out in THF with double presaturation by the addition of an about 1 mM [Zn$_2$(L)] and about 12 mM ^{n}Bu$_4$N.Cl solution to an about 1 mM [Zn$_2$(L)] solution, or in pyridine-d_5 by addition of an about 16 mM [Zn$_2$(L)] and about 195 mM ^{n}Bu$_4$N.Cl solution to an about 16 mM [Zn$_2$(L)] solution (in each case, the highest concentration was limited by the solubility of [Zn$_2$(L)]).

Microcalorimetric Titrations. Titrations were carried out by the automated sequential addition of the salt solution to a [Zn$_2$(L)] solution at 298 K. Extensive efforts were made to exclude moisture from the sample as this could decompose the binuclear zinc complex, weaken the receptor-anion interactions, and result in preferential binding of OH$^-$. Host solutions were prepared under argon atmosphere in glovebox at least 16 h in advance to allow full dissolution, stored under argon and used within 24 h of opening. The guest samples were also prepared with dry solvents and used within 12 h. For each anion investigated, at least three concordant titrations were carried out with different host and guest concentrations (typically 1 or 0.5 mM and 10 or 20 mM respectively).

Calculations. >Initial structures of the ligand and ligand-anion complexes were built using ArgusLab,[30] based on the crystal structure of the binuclear palladium complex [Pd$_2$(L)], and used as starting points for unconstrained geometry optimizations. The absence of imaginary frequencies was used to confirm that each calculated structure was a minimum on the molecular potential energy surface. All calculations were carried out using Gaussian09,[31] running under Linux. Geometry optimizations and binding energy calculations were conducted at several levels of theory. Initial calculations employed Becke's popular three parameter exchange functional[32] coupled with the Lee−Yang−Parr[33] correlation functional (B3LYP) in combination with the LANL2DZ basis set of Hay and Wadt,[34] which comprises an effective core potential (ECP) plus double-ζ basis for heavy atoms, with the all-electron valence double-ζ basis set developed by Dunning (D95 V) for lighter atoms.[35] This basis set was chosen primarily because of the size of the complexes under study and the need to balance accuracy with computational cost, and, second, to satisfy the requirement for a balanced basis set spanning the atomic range from hydrogen to iodine. Comparative calculations using Pople's[36] 6-31 g(d.p) basis set (which includes polarization functions on all atoms) for the chloride, hydroxide and bromide complexes (it is not available for iodine) were undertaken to investigate the effect of basis set size on the calculated binding energies, which were observed to differ by at most 2 kcal mol^{-1} (Table 2). Thus, the less computationally demanding LANL2DZ basis set was favored. Both B3LYP/LANL2DZ and B3LYP/6-31 g(d,p) have been shown to predict calculated structures in good agreement with those determined experimentally for large organometallic compounds.[37] However, the improper inclusion of dispersion interactions within B3LYP is of concern in the study of noncovalently bound complexes, such as those in this work. As a comparison the M05−2X functional of Zhao and Truhlar,[38]which has been shown to recover significantly more midrange correlation than B3LYP,[39] at a similar computational cost was also tested, again, in combination with the LANL2DZ basis set. Bulk solvent interactions were modeled via the self-consistent reaction field (SCRF) using the polarizable continuum model (PCM),[40] employing the default parameters for THF within Gaussian 09.

Ligand-anion binding energies were calculated using:

$$\Delta E = E[[\mathrm{Zn_2}(\mu\text{-X})(\mathrm{L})] + \mathrm{ZPE}] - E[[\mathrm{Zn_2}(\mathrm{L})] + \mathrm{ZPE}] - E[(\mathrm{X})] + \mathrm{BSSE}$$

where $E[$Zn$_2(\mu$-X)(L)$]$ is the energy of the solvated host:guest complex, $E[$Zn$_2$(L)$]$ is the energy of the solvated complex alone, E[X] is the energy of the solvated anionic species, and the ZPE are the appropriate zero-point energy corrections for each component. The counterpoise method of Boys and Bernardi[41] was employed to correct for basis set superposition errors (BSSE) in the calculated binding energies, arising as a consequence of the incompleteness of the basis set.

■ ASSOCIATED CONTENT

Supporting Information. X-ray crystal structure of [Li(THF)$_4$][Zn$_2(\mu$-OH)(L)], Figures S1−S4, Tables S1−2, xyx coordinates for the calculated structures. This material is available free of charge via the Internet at http://pubs.acs.org.

Present Addresses
[§]Department of Chemistry, Yonsei University, Seoul, 120-749, Korea.

AUTHOR INFORMATION

Corresponding Author
*E-mail: jason.love@ed.ac.uk.

ACKNOWLEDGMENT

The authors thank EaStCHEM, the University of Edinburgh, EPSRC(UK), and the National Institutes of Health (Grant CA 68682 to J.L.S.) for funding, Dr. P. Barran and M. De Cecco at the University of Edinburgh for help with the nano-ESIMS, and the Cowley group at the University of Texas in Austin for the use of glovebox facilities. This work has made use of the resources provided by the EaStCHEM Research Computing Facility, (http://www.eastchem.ac.uk/rcf) and the Edinburgh Compute and Data Facility (ECDF). (http://www.ecdf.ed.ac.uk/). Both facilities are partially supported by the eDIKT initiative. (http://www.edikt.org.) Acknowledgment is also made to the Robert A. Welch Foundation (grant F-1018 to J.L.S.) and the Korean WCU program (grant R32-2008-000-10217-0 for J.L.S.).

REFERENCES

(1) Gale, P. A.; Gunnlaugsson, T. *Chem. Soc. Rev.* **2010**, *39*, 3595.Sessler, J. L.; Gale, P. A.; Cho, W.-S. *Anion Receptor Chemistry*; Royal Society of Chemistry: Cambridge, U.K., 2006.

(2) Paiva, A. P.; Malik, P. *J. Radionucl. Nucl. Chem.* **2004**, *261*, 485.

(3) Coxall, R. A.; Lindoy, L. F.; Miller, H. A.; Parkin, A.; Parsons, S.; Tasker, P. A.; White, D. J. *Dalton Trans.* **2003**, 55. Plieger, P. G.; Parsons, S.; Parkin, A.; Tasker, P. A. *J. Chem. Soc., Dalton Trans.* **2002**, 3928. Wenzel, M.; Jameson, G. B.; Ferguson, L. A.; Knapp, Q. W.; Forgan, R. S.; White, F. J.; Parsons, S.; Tasker, P. A.; Plieger, P. G. *Chem. Commun.* **2009**, 3606. Gasperov, V.; Galbraith, S. G.; Lindoy, L. F.; Rumbel, B. R.; Skelton, B. W.; Tasker, P. A.; White, A. H. *Dalton Trans.* **2005**, 139. Forgan, R. S.; Davidson, J. E.; Fabbiani, F. P. A.; Galbraith, S. G.; Henderson, D. K.; Moggach, S. A.; Parsons, S.; Tasker, P. A.; White, F. J. *Dalton Trans.* **2010**, *39*, 1763. Galbraith, S. G.; Lindoy, L. F.; Tasker, P. A.; Plieger, P. G. *Dalton Trans.* **2006**, 1134.

(4) Ballester, P. *Chem. Soc. Rev.* **2010**, *39*, 3810. Dalla Cort, A.; De Bernardin, P.; Forte, G.; Yafteh Mihan, F. *Chem. Soc. Rev.* **2010**, *39*, 3863. Kang, S. O.; Llinares, J. M.; Day, V. W.; Bowman-James, K. *Chem. Soc. Rev.* **2010**, *39*, 3980. Kim, S. K.; Sessler, J. L. *Chem. Soc. Rev.* **2010**, *39*, 3784. Mercer, D. J.; Loeb, S. J. *Chem. Soc. Rev.* **2010**, *39*, 3612. Steed, J. W. *Chem. Soc. Rev.* **2009**, *38*, 506. O'Neil, E. J.; Smith, B. D. *Coord. Chem. Rev.* **2006**, *250*, 3068. Amendola, V.; Bonizzoni, M.; Esteban-Gómez, D.; Fabbrizzi, L.; Licchelli, M.; Sancenón, F.; Taglietti, A. *Coord. Chem. Rev.* **2006**, *250*, 1451. Vilar, R. *Eur. J. Inorg. Chem.* **2008**, *2008*, 357. Rice, C. R. *Coord. Chem. Rev.* **2006**, *250*, 3190.Sessler, J. L., 2006; Suksai, C.; Tuntulani, T. *Chem. Soc. Rev.* **2003**, *32*, 192. Beer, P. D.; Hayes, E. J. *Coord. Chem. Rev.* **2003**, *240*, 167.Bayly, S.; Beer, P., . In *Recognition of Anions*; Springer: Berlin, Germany, 2008; pp 45.

(5) Beer, P. D.; Cormode, D. P.; Davis, J. J. *Chem. Commun.* **2004**, 414.

(6) Amendola, V.; Fabbrizzi, L.; Mangano, C.; Pallavicini, P.; Poggi, A.; Taglietti, A. *Coord. Chem. Rev.* **2001**, *219*−*221*, 821.

(7) Jacques, B.; Dro, C.; Bellemin-Laponnaz, S.; Wadepohl, H.; Gade, L. H. *Angew. Chem., Int. Ed.* **2008**, *47*, 4546. Carvalho, S.; Delgado, R.; Drew, M. G. B.; Felix, V. *Dalton Trans.* **2007**, 2431. Chen, Z.-h.; He, Y.-b.; Hu, C.-G.; Huang, X.-h. *Tetrahedron: Asymmetry* **2008**, *19*, 2051. Goswami, S.; Chakrabarty, R. *Tetrahedron Lett.* **2009**, *50*, 5994. Shen, R.; Pan, X.; Wang, H.; Wu, J.; Tang, N. *Inorg. Chem. Commun.* **2008**, *11*, 318. Mattigod, S. V.; Fryxell, G. E.; Parker, K. E. *Inorg. Chem. Commun.* **2007**, *10*, 646. Min, Su, H.; Dong, H. K. *Angew. Chem., Int. Ed.* **2002**, *41*, 3809. Mizukami, S.; Nagano, T.; Urano, Y.; Odani, A.; Kikuchi, K. *J. Am. Chem. Soc.* **2002**, *124*, 3920. Stastny, V.; Lhoták, P.; Stibor, I.; König, B. *Tetrahedron* **2006**, *62*, 5748. Kim, K.-H.; Park, J. S.; Kang, T. Y.; Oh, K.; Seo, M.-S.; Sohn, Y. S.; Jun, M.-J.; Nam, W.; Kim, K. M. *Chem.—Eur. J.* **2006**, *12*, 7078. Boiocchi, M.; Fabbrizzi, L.; Garolfi, M.; Licchelli, M.; Mosca, L.; Zanini, C. *Chem.—Eur. J.* **2009**, *15*, 11288. Sabiah, S.; Varghese, B.; Murthy, N. N. *Chem. Commun.* **2009**, 5636. Ganesh, V.; Sanz, M. P. C.; Mareque-Rivas, J. C. *Chem. Commun.* **2007**, 5010. Love, J. B.; Vere, J. M.; Glenny, M. W.; Blake, A. J.; Schröder, M. *Chem. Commun.* **2001**, 2678.

(8) Champouret, Y. D. M.; Nodes, W. J.; Scrimshire, J. A.; Singh, K.; Solan, G. A.; Young, I. *Dalton Trans.* **2007**, 4565. Roy, P.; Dhara, K.; Manassero, M.; Banerjee, P. *Inorg. Chim. Acta* **2009**, *362*, 2927. Fontecha, J. B.; Goetz, S.; McKee, V. *Dalton Trans.* **2005**, 923. McDonough, M. J.; Reynolds, A. J.; Lee, W. Y. G.; Jolliffe, K. A. *Chem. Commun.* **2006**, 2971. Ganesh, V.; Sanz, M. P. C.; Mareque-Rivas, J. C. *Chem. Commun.* **2007**, 804. Ambrosi, G.; Formica, M.; Fusi, V.; Giorgi, L.; Guerri, A.; Macedi, E.; Micheloni, M.; Paoli, P.; Pontellini, R.; Rossi, P. *Inorg. Chem.* **2009**, *48*, 5901.

(9) Lehn, J. M.; Pine, S. H.; Watanabe, E.; Willard, A. K. *J. Am. Chem. Soc.* **1977**, *99*, 6766.

(10) Chen, J.-M.; Zhuang, X.-M.; Yang, L.-Z.; Jiang, L.; Feng, X.-L.; Lu, T.-B. *Inorg. Chem.* **2008**, *47*, 3158.

(11) Harding, C. J.; Mabbs, F. E.; MacInnes, E. J. L.; McKee, V.; Nelson, J. *J. Chem. Soc., Dalton Trans.* **1996**, *15*, 3227.

(12) Jang, H. H.; Yi, S.; Kim, M. H.; Kim, S.; Lee, N. H.; Han, M. S. *Tetrahedron Lett.* **2009**, *50*, 6241. Smith, B. A.; Akers, W. J.; Leevy, W. M.; Lampkins, A. J.; Xiao, S.; Wolter, W.; Suckow, M. A.; Achilefu, S.; Smith, B. D. *J. Am. Chem. Soc.* **2009**, *132*, 67. Ojida, A.; Takashima, I.; Kohira, T.; Nonaka, H.; Hamachi, I. *J. Am. Chem. Soc.* **2008**, *130*, 12095. Leevy, W. M.; Gammon, S. T.; Jiang, H.; Johnson, J. R.; Maxwell, D. J.; Jackson, E. N.; Marquez, M.; Piwnica-Worms, D.; Smith, B. D. *J. Am. Chem. Soc.* **2006**, *128*, 16476. Coggins, M., K; Parker, A., M; Mangalum, A.; Galdamez, G., A; Smith, R., C *Eur. J. Org. Chem.* **2009**, *2009*, 343. Khatua, S.; Choi, S. H.; Lee, J.; Kim, K.; Do, Y.; Churchill, D. G. *Inorg. Chem.* **2009**, *48*, 2993. Feng, G.; Natale, D.; Prabaharan, R.; Mareque-Rivas, J. C.; Williams, N. H. *Angew. Chem., Int. Ed.* **2006**, *45*, 7056. Jang, Y. J.; Jun, E. J.; Lee, Y. J.; Kim, Y. S.; Kim, J. S.; Yoon, J. *J. Org. Chem.* **2005**, *70*, 9603. DiVittorio, K. M.; Leevy, W. M.; O'Neil, E. J.; Johnson, J. R.; Vakulenko, S.; Morris, J. D.; Rosek, K. D.; Serazin, M.; Hilkert, S.; Hurley, S.; Marquez, M.; Smith, B. D. *ChemBioChem* **2008**, *9*, 286. Lee, D. H.; Im, J. H.; Son, S. U.; Chung, Y. K.; Hong, J.-I. *J. Am. Chem. Soc.* **2003**, *125*, 7752. Lee, H. N.; Swamy, K. M. K.; Kim, S. K.; Kwon, J.-Y.; Kim, Y.; Kim, S.-J.; Yoon, Y. J.; Yoon, J. *Org. Lett.* **2006**, *9*, 243. Lee, J. H.; Park, J.; Lah, M. S.; Chin, J.; Hong, J.-I. *Org. Lett.* **2007**, *9*, 3729.

(13) Champouret, Y. D. M.; Fawcett, J.; Nodes, W. J.; Singh, K.; Solan, G. A. *Inorg. Chem.* **2006**, *45*, 9890. Singh, N.; Jung, H. J.; Jang, D. O. *Tetrahedron Lett.* **2009**, *50*, 71.

(14) Beletskaya, I.; Tyurin, V. S.; Tsivadze, A. Y.; Guilard, R.; Stern, C. *Chem. Rev.* **2009**, *109*, 1659.

(15) Lee, C.; Lee, D. H.; Hong, J.-I. *Tetrahedron Lett.* **2001**, *42*, 8665. Cormode, D. P.; Drew, M. G. B.; Jagessar, R.; Beer, P. D. *Dalton Trans.* **2008**, 6732. Bucher, C.; Devillers, C. H.; Moutet, J.-C.; Royal, G.; Saint-Aman, E. *New J. Chem.* **2004**, *28*, 1584.

(16) Rosenthal, J.; Nocera, D. G. *Prog. Inorg. Chem.* **2007**, *55*, 483. Rosenthal, J.; Nocera, D. G. *Acc. Chem. Res.* **2007**, *40*, 543. Harvey, P. D.; Stern, C.; Gros, C. P.; Guilard, R. *Coord. Chem. Rev.* **2007**, *251*, 401. Collman, J. P.; Wagenknecht, P. S.; Hutchinson, J. E. *Angew. Chem., Int. Ed.* **1994**, *33*, 1537.

(17) Jokic, D.; Boudon, C.; Pognon, G.; Bonin, M.; Schenk, K., J.; Gross, M.; Weiss, J. *Chem.—Eur. J.* **2005**, *11*, 4199. Yagi, S.; Ezoe, M.; Yonekura, I.; Takagishi, T.; Nakazumi, H. *J. Am. Chem. Soc.* **2003**, *125*, 4068. Oliveri, C. G.; Gianneschi, N. C.; Nguyen, S. T.; Mirkin, C. A.; Stern, C. L.; Wawrzak, Z.; Pink, M. *J. Am. Chem. Soc.* **2006**, *128*, 16286. Oliveri, C. G.; Ulmann, P. A.; Wiester, M. J.; Mirkin, C. A. *Acc. Chem. Res.* **2008**, *41*, 1618. Chi-Hwa, L.; Hongsik, Y.; Woo-Dong, J. *Chem.—Eur. J.*

2009, *15*, 9972. Brettar, J.; Gisselbrecht, J.-P.; Gross, M.; Solladie, N. *Chem. Commun.* **2001**, 733. Hunter, C. A.; Meah, M. N.; Sanders, J. K. M. *J. Am. Chem. Soc.* **1990**, *112*, 5773. Rein, R.; Gross, M.; Solladie, N. *Chem. Commun.* **2004**, 1992. Ballester, P.; Costa, A.; Castilla, A. M.; Deyà, P. M.; Frontera, A.; Gomila, R. M.; Hunter, C. A. *Chem.—Eur. J.* **2005**, *11*, 2196. Zhou, Z.-C.; He, L.; Zhu, Y.-Z.; Zheng, J.-Y. *Chin. J. Chem.* **2007**, *25*, 1632.

(18) Kim, D.; Lee, S.; Gao, G.; Seok Kang, H.; Ko, J. *J. Organomet. Chem.* **2010**, *695*, 111. Bampos, N.; Marvaud, V.; Sanders, J. K. M. *Chem.—Eur. J.* **1998**, *4*, 335.

(19) Gal, M.; Marzin, C.; Tarrago, G.; Zidane, I.; Hours, T.; Lerner, D.; Andrieux, C.; Gampp, H.; Saveant, J. M. *Inorg. Chem.* **1986**, *25*, 1775. Muraoka, T.; Kinbara, K.; Aida, T. *J. Am. Chem. Soc.* **2006**, *128*, 11600. Carofiglio, T.; Lubian, E.; Menegazzo, I.; Saielli, G.; Varotto, A. *J. Org. Chem.* **2009**, *74*, 9034. Zhou, Z.-C.; Zhu, Y.-Z.; Zheng, J.-Y. *Sci. China B: Chem.* **2009**, *52*, 1353. Tabushi, I.; Kugimiya, S. *J. Am. Chem. Soc.* **1986**, *108*, 6926. Tabushi, I.; Kugimiya, S.; Sasaki, T. *J. Am. Chem. Soc.* **1985**, *107*, 5159.

(20) Li, X.; Tanasova, M.; Vasileiou, C.; Borhan, B. *J. Am. Chem. Soc.* **2008**, *130*, 1885. Marina, T.; Chrysoula, V.; Oluwatoyin, O. O.; Babak, B. *Chirality* **2009**, *21*, 374.

(21) Tashiro, K.; Aida, T. *Chem. Soc. Rev.* **2007**, *36*, 189. Shoji, Y.; Tashiro, K.; Aida, T. *Chirality* **2008**, *20*, 420. Tong, L., H.; Wietor, J.-L.; Clegg, W.; Raithby, P., R.; Pascu, S., I.; Sanders, J. K. M. *Chem.—Eur. J.* **2008**, *14*, 3035. Hosseini, A.; Taylor, S.; Accorsi, G.; Armaroli, N.; Reed, C. A.; Boyd, P. D. W. *J. Am. Chem. Soc.* **2006**, *128*, 15903. Sun, D.; Tham, F. S.; Reed, C. A.; Chaker, L.; Burgess, M.; Boyd, P. D. W. *J. Am. Chem. Soc.* **2000**, *122*, 10704. Yanagisawa, M.; Tashiro, K.; Yamasaki, M.; Aida, T. *J. Am. Chem. Soc.* **2007**, *129*, 11912. Shoji, Y.; Tashiro, K.; Aida, T. *J. Am. Chem. Soc.* **2006**, *128*, 10690.

(22) Givaja, G.; Blake, A. J.; Wilson, C.; Schröder, M.; Love, J. B. *Chem. Commun.* **2003**, 2508. Sessler, J. L.; Cho, W.-S.; Dudek, S. P.; Hicks, L.; Lynch, V. M.; Huggins, M. T. *J. Porphyrins Phthalocyanines* **2003**, *7*, 97. Love, J. B. *Chem. Commun.* **2009**, 3154.

(23) Givaja, G.; Volpe, M.; Edwards, M. A.; Blake, A. J.; Wilson, C.; Schröder, M.; Love, J. B. *Angew. Chem., Int. Ed.* **2007**, *46*, 584. Volpe, M.; Hartnett, H.; Leeland, J. W.; Wills, K.; Ogunshun, M.; Duncombe, B.; Wilson, C.; Blake, A. J.; McMaster, J.; Love, J. B. *Inorg. Chem.* **2009**, *48*, 5195.

(24) Askarizadeh, E.; Devoille, A. M. J.; Boghaei, D. M.; Slawin, A. M. Z.; Love, J. B. *Inorg. Chem.* **2009**, *48*, 7491.

(25) Faure, S.; Stern, C.; Guilard, R.; Harvey, P. D. *J. Am. Chem. Soc.* **2004**, *126*, 1253.

(26) Osuka, A.; Nakajima, S.; Nagata, T.; Maruyama, K.; Toriumi, K. *Angew. Chem., Int. Ed. Engl.* **1991**, *30*, 582. Chang, C. J.; Deng, Y.; Heyduk, A. F.; Chang, C. K.; Nocera, D. G. *Inorg. Chem.* **2000**, *39*, 959. Deng, Y.; Chang, C. J.; Nocera, D. G. *J. Am. Chem. Soc.* **1999**, *122*, 410.

(27) Allen, F. *Acta Crystallogr., Sect. B* **2002**, *58*, 380.

(28) Lachkar, M.; Tabard, A.; Brandes, S.; Guilard, R.; Atmani, A.; De Cian, A.; Fischer, J.; Weiss, R. *Inorg. Chem.* **1997**, *36*, 4141.

(29) Balaban, T. S.; Goddard, R.; Linke-Schaetzel, M.; Lehn, J.-M. *J. Am. Chem. Soc.* **2003**, *125*, 4233. Balaban, T. S.; Linke-Schaetzel, M.; Bhise, Anil, D.; Vanthuyne, N.; Roussel, C. *Eur. J. Org. Chem.* **2004**, *2004*, 3919.

(30) Thompson, M. A. *ArgusLab*, 4.0.1; Planaria Software LLC: Seattle, WA; http://www.arguslab.com.

(31) Frisch, M. J.; Trucks, G. W.; Schlegel, H. B.; Scuseria, G. E.; Robb, M. A.; Cheeseman, J. R.; Scalmani, G.; Barone, V.; Mennucci, B.; Petersson, G. A.; Nakatsuji, H.; Caricato, M.; Li, X.; Hratchian, H. P.; Izmaylov, A. F.; Bloino, J.; Zheng, G.; Sonnenberg, J. L.; Hada, M.; Ehara, M.; Toyota, K.; Fukuda, R.; Hasegawa, J.; Ishida, M.; Nakajima, T.; Honda, Y.; Kitao, O.; Nakai, H.; Vreven, T.; Montgomery Jr., J. A.; Peralta, J. E.; Ogliaro, F.; Bearpark, M.; Heyd, J. J.; Brothers, E.; Kudin, K. N.; Staroverov, V. N.; Kobayashi, R.; Normand, J.; Raghavachari, K.; Rendell, A.; Burant, J. C.; Iyengar, S. S.; Tomasi, J.; Cossi, M.; Rega, N.; Millam, N. J.; Klene, M.; Knox, J. E.; Cross, J. B.; Bakken, V.; Adamo, C.; Jaramillo, J.; Gomperts, R.; Stratmann, R. E.; Yazyev, O.; Austin, A. J.; Cammi, R.; Pomelli, C.; Ochterski, J. W.; Martin, R. L.; Morokuma, K.; Zakrzewski, V. G.; Voth, G. A.; Salvador, P.; Dannenberg, J. J.; Dapprich, S.; Daniels, A. D.; Farkas, Ö.; Foresman, J. B.; Ortiz, J. V.; Cioslowski, J.; Fox, D. J. *Gaussian 09*, Revision A.02; Gaussian Inc.: Wallingford, CT, 2009.

(32) Becke, A. D. *J. Chem. Phys.* **1993**, *98*, 5648.

(33) Lee, C.; Yang, W.; Parr, R. G. *Phys. Rev. B* **1988**, *37*, 785.

(34) Hay, P. J.; Wadt, W. R. *J. Chem. Phys.* **1985**, *82*, 270. Hay, P. J.; Wadt, W. R. *J. Chem. Phys.* **1985**, *82*, 299. Hay, P. J.; Wadt, W. R. *J. Chem. Phys.* **1985**, *82*, 284.

(35) Dunning Jr., T. H.; Hay, P. J. In *Modern Theoretical Chemistry*; Schaefer, H. F., III, Ed.; Plenum: New York, 1976; Vol. 3, p 1.

(36) Ditchfield, R.; Hehre, W. J.; Pople, J. A. *J. Chem. Phys.* **1971**, *54*, 724.

(37) Lin, J.-G.; Qiu, L.; Xu, Y.-Y. *Bull. Korean Chem. Soc.* **2009**, *30*, 1021. Linfoot, C. L.; Richardson, P. R.; Hewat, T. E.; Moudam, O.; Forde, M. M.; Collins, A.; White, F. J.; Robertson, N. *Dalton Trans.* **2010**, *39*, 8945.

(38) Zhao, Y.; Schultz, N. E.; Truhlar, D. G. *J. Chem. Theory Comput.* **2006**, *2*, 364.

(39) Zhao, Y.; Truhlar, D. G. *J. Chem. Theory Comput.* **2007**, *3*, 289. Wong, B. M. *J. Comput. Chem.* **2008**, *30*, 289.

(40) Miertuš, S.; Scrocco, E.; Tomasi, J. *Chem. Phys.* **1981**, *55*, 117.

(41) Boys, S. F.; Bernadi, F. *Mol. Phys.* **1970**, *19*, 533.